Extraction of Spray Particles with Supercritical Fluids in a Two-Phase Flow

Henning Wagner and Rudolf Eggers
Dept. Verfahrenstechnik II, Technische Universität Hamburg-Harburg, 21071 Hamburg, Germany

A new process for extractive separation with supercritical fluids is described. It is characterized by mixing a liquid feed with a dense gas in a special mixing device and the formation of spray particles when this mixture is injected into an extraction zone where the fluid phase is loaded with the extracts. By dividing the extraction into two process steps, mixing and loading, it is possible to adjust the devices and apparatuses for different media. For example, a static mixer or a fluid-assist atomizer can be used as mixing devices. Since the viscosity behavior of the mixture and the surface tension in dense gases are important for the formation of spray particles, carbon dioxide was measured at pressures up to 70 MPa and the geometry of the extraction zone was optimized by residence times and fluid dynamics.

Two different materials were tested in an apparatus on a semiindustrial scale with different mixing devices and extraction zones. By measuring fluid loading in the extraction zone, the mass-transfer parameter of a mathematical extraction model could be adapted. The model considers particle formation in the mixing zone, the fluid dynamic in the loading zone, and the mass transfer between spray particles and fluid phase. Calculated concentration profiles make it possible to determine the residence time and the size of the extraction zone for given geometries and fluid dynamics.

Introduction

Extraction processes using supercritical fluids have been used for several solids extractions such as decaffination, hops extraction, and extraction of scents and essential oils. They often replace processes using organic solvents. In addition to solids extraction, liquid extraction has been of special interest in recent years because a continuous process is possible in countercurrent high-pressure columns. Some problems involving the extractive treatment of multicomponent liquid systems with supercritical CO_2 can cause a high number of transfer particles in countercurrent high-pressure columns and result in an uneconomical process:

1. The high rate of resistance of the separating component to mass transfer. This is caused by: (a) a low diffusion coefficient in the liquid solvent (e.g., aqueous or highly viscous systems); (b) solidification of the raffinate (analogous to spray drying processes).

2. Unfavorable distribution equilibrium because of separating components with low solubility in the supercritical phase.

3. The separation of the extract is superimposed on a small scale by the solubility of the liquid solvent in the supercritical fluid.

In this study the fundamental idea developed to solve such separation problems is a decrease in the mass-transfer resistance in the liquid phase by an extreme reduction of the diffusion paths with a simultaneous increase in the mass transfer surface. Both effects can be reached by a drop dispersion of the liquid in the fluid (supercritical) phase. The desired drop dispersion is generated in a spraying device, and the resulting two-phase mixture is sprayed into an extraction chamber.

In a spraying device like a fluid-assist atomizer the following effects lead to the generation of very small drops and an increase in the mass-transfer rate:

1. The high kinetic energy of the compressed fluid breaks a liquid filament.

Correspondence concerning this article should be addressed to Prof. Dr.-Ing. R. Eggers.

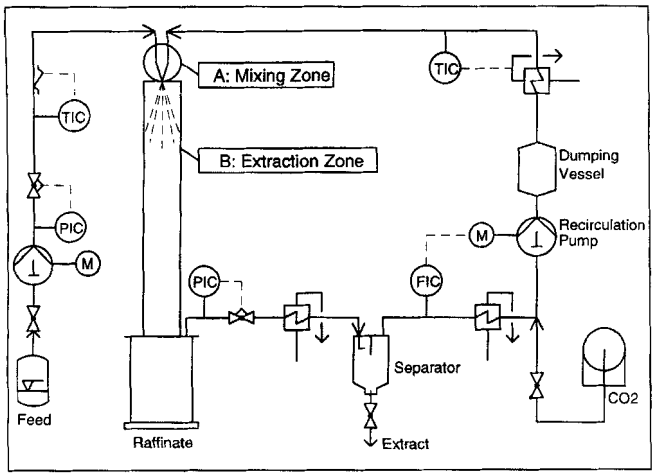

Figure 1. Representation of the apparatus on a semi-industrial scale.

2. The surface tension in CO_2 is strongly reduced, resulting in an increase in the boundary surface between the liquid and the fluid.

3. Liquids with dissolved CO_2 show a strong reduction in viscosity. This reduces the necessary atomization impulse as well as the mass-transfer resistance of the liquid phase.

The jet extraction suggested by Stahl and Quirin (1985), which has been proposed especially for the deoiling of lecithin, is the basis of the spray extraction. A process was developed on a semi-industrial scale and was described in detail by Eggers and Wagner (1993). An apparatus like that in Figure 1 was used. The liquid feed was compressed by a reciprocating pump and fed into a mixing zone, where it is mixed with and dispersed by highly agitated CO_2. Thus, a part of the kinetic energy of the CO_2 is used to increase the surfaces in order to achieve very small drops. The resulting two-phase flow runs through an extraction zone, where uniform extraction at very short diffusion paths occurs, and the fluid phase is loaded with the separating components. The liquid extract or raffinate is collected in a vessel while the loaded CO_2 is expanded through a pneumatically controlled high-pressure butterfly valve into the separation stage. Changing pressure and temperature causes the CO_2 to lose solubility, which allows the extract to fall out. Raffinates can be continuously released, while solid materials need to be collected as a batch. The recompression of the CO_2, which is liquidized in a cooler, is carried out in a triple-cylinder plunger pump with a low stagnant volume proportion. This, together with a damping vessel, guarantees that a discontinuity in the CO_2 flow can be excluded. The apparatus can be used on a semi-industrial scale for extraction pressures up to 90 MPa and temperatures up to 413 K. Under these extraction conditions the pump for the circulating CO_2 allows a maximum fluid flow of 125 kg/h.

The objective of this study is to show how the two process steps, "mixing" (drop dispersion) and "loading" (extraction), can be adapted and optimized separately for materials with different extraction behaviors. It distinguishes between the extraction of liquid drops and that of solid particles. As liquid substances for the model, two quasi binary mixtures of nonpolar soy soil and polar phospholipids have been chosen. Soy oil is a soluble component, while the phospholipids are completely insoluble in CO_2. Therefore, this system shows a high separation factor and is especially suitable for studying the process.

Only stable mixtures of oil and phospholipids could be used in this study. In commercial soy oil processing there are two of these:

1. Crude soy oil, which contains about 3 wt. % phospholipids. In production, these latter are separated as lecithin by a hydration process.

2. Lecithin, which contains about 65 wt. % phospholipids. This result is produced by hydration.

The viscosity of lecithin is much higher than that of crude oil, but both show a similar surface tension in CO_2. The valuable products of lecithin extraction are the deoiled phospholipids that are collected as a powdery solid raffinate. In contrast to this, the extraction of crude oil should produce a deslimed oil as a liquid extract. Contact of the sprayed lecithin drops with CO_2 causes rapid formation of *solid* particles. Sprayed crude oil, however, is extracted as *liquid* drops.

Because both mixtures used in the model contain the same single components, which behave similarly in solubility and surface tension, as well as a similar separation factor, the investigation focuses on the theoretical and practical aspects of the formation of spray particles in dense gases, the influence of the dynamics of the two-phase flow on the extraction zone, and different numerical models describing the mass transfer from liquid drops and solid particles to fluid phases.

Design of the Apparatus

The geometrical design of the mixing and extraction zones determines the flow dynamics in the apparatus, and therefore the spray particle formation as well as the extractive mass transfer. Suitable designs for mixing and extraction depend on the properties and the extraction behavior of the liquids.

Mixing zone

Spraying devices or elements of a static mixer, which are set into a pressure tube, can be used to mix the liquid into the fluid. The liquid viscosity is the main criterion in selecting a mixing principle. Different designs for mixing devices are shown as sectional drawings in Figure 2.

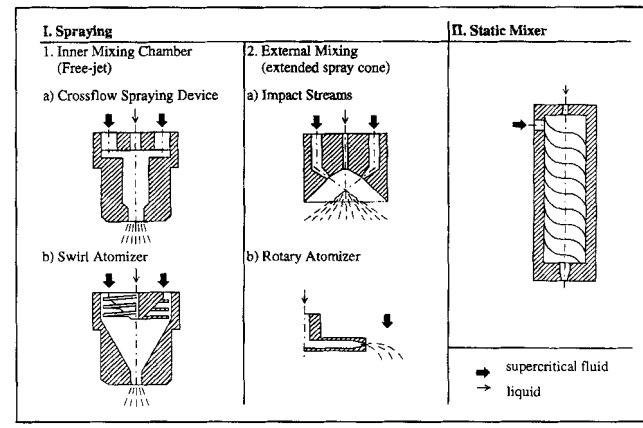

Figure 2. Designs of mixing devices.

The crossflow spraying device is especially suited for highly viscous materials, because the momentum of the CO_2 stream is brought directly on a liquid filament crosswise to its outlet. In a swirl atomizer it is possible to create a spin momentum by the fluid flow on liquids with low viscosity. The addition of tangential velocity streams increases the convective mass transfer in the subsequent two-phase flow. Both spraying devices have an inner mixing chamber where the drops are formed at extremely high Reynolds numbers (*Re*) of more than 10^5. Spray particles leaving the outlet of these inner mixing chambers form a spray cone similar to a free jet with an angle between 15° and 20°.

Spray devices with external mixing and extended spray cone can be used for low-viscosity liquids. These spray cones distribute the spray particles more evenly in the geometry of the extraction zone. Examples of external mixing are the spraying of two impact streams and a rotary atomizer with a bell-shaped spray cone. If the mixing is done in a static mixer, the viscosity of the liquid is reduced, so that a plain orifice might be adequate to spray the mixture into the extraction zone.

In the applied apparatus it was possible to test spraying devices by forming a free jet. Spraying devices with an extended spray cone need extraction zones with a large diameter (see below), but these were not available until now. So, the crossflow device with an inner mixing chamber described here was used for the high viscosity lecithin, while the crude oil could be sprayed by this device as well as by the swirl atomizer shown in Figure 2.

Extraction zone

When selecting the shape of the extraction zone, the designer must consider particle formation during extraction. Some possible designs for the extraction zone are shown in Figure 3. During extraction the *liquid* drops cannot be allowed to reach the shape's perimeter, because this would cause a liquid film with strongly reduced mass transfer surface.

Only materials forming *solid* particles immediately after spraying can be extracted in a tube with a relatively small diameter. In this study, solids extraction is accomplished by deoiling lecithin in a tube with an inner diameter of 14.3 mm at *Re* numbers between 30,000 and 50,000. The tube is 4 m long, so the lecithin particles are extracted at residence times at 15 s to 30 s.

For substances that are extracted as *liquid* drops, the extraction should occur only while the spray particles are in the spray cone. A cone-shaped extraction zone is ideal for this, but this shape is not used in vessel construction. Instead, a cylinder with a larger diameter or a spherical vessel serves as a realizable design; a spherical vessel is especially useful for spraying devices with a bell-shaped spray. While experiments for deoiling lecithin are done in a tube, the desliming of crude oil could be carried out in a high-pressure extraction vessel with an inner diameter of 50 mm. A free-jet spray cone reaches the wall first at a distance of about 200 mm from the spraying device. The substance remains in this spray cone for about 6 s.

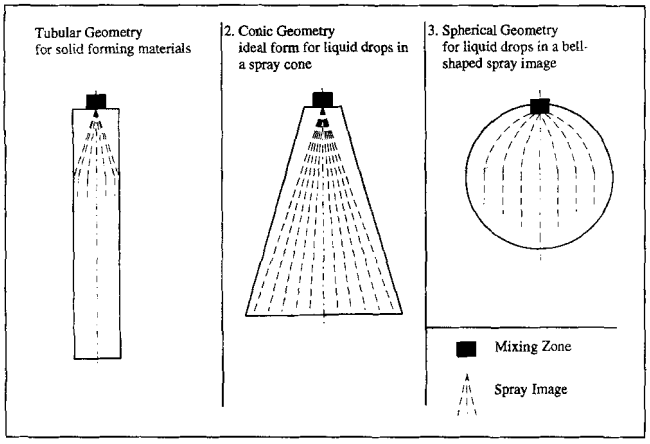

Figure 3. Possible designs for the extraction zone.

Formulation of a Model

A mathematical model of drop formation and extractive mass transfer is necessary in order to optimize the mixing and the extraction zones, which are considered separately for different liquids, depending on the extraction conditions. Figure 4 shows the spray extraction process with four sections: 1. mixing/drop dispersion; 2. flow dynamics in the spray cone; 3. transition of the spray cone to the pipe flow; and 4. fully developed pipe flow. Only the first two items are relevant for

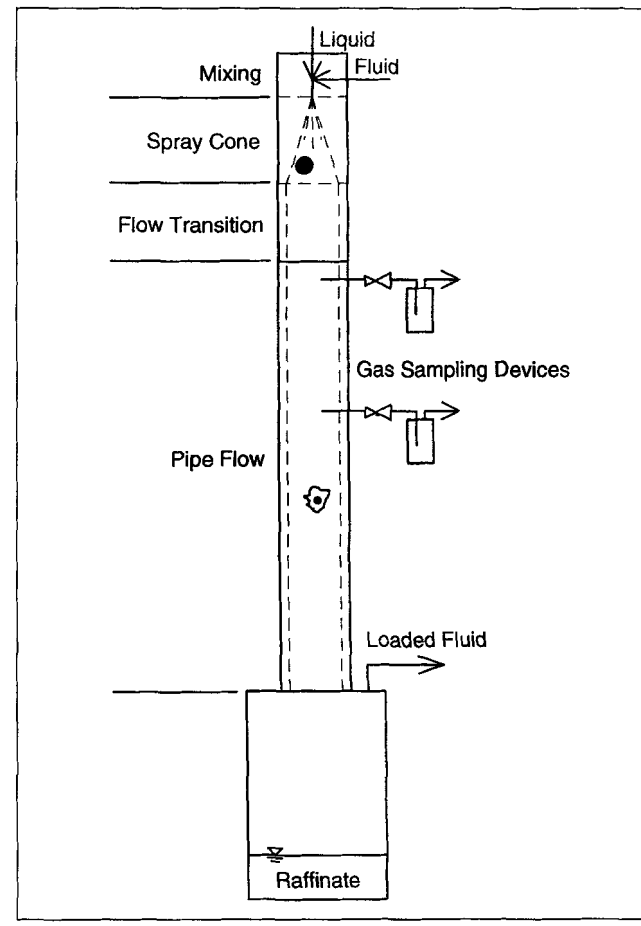

Figure 4. Representation of the spray extraction process.

the extraction of *liquid* drops, while the last two apply to *solid* particle extraction. The modeling results can be verified by measuring the fluid loading in the extraction tube used for the deoiling of lecithin (extraction of solid particles). Therefore, gas-sampling devices are set into the extraction tube at two different distances from the spray formation. Together with the inlet conditions and the oil contents in the raffinate, a profile of the fluid loading can be established over the entire length of the extraction zone.

The drop-size distribution formed in the spraying device can be described by dimensionless characteristic numbers. These characteristic numbers are dependent on the fluid and liquid properties at extraction conditions. The density of CO_2 can be calculated with the Bender equation, which is listed by Sievers (1984). An analog for the viscosity of CO_2 is given by Chung et al. (1988). The behavior of viscosity and surface tension for lecithin and crude oil needed to be measured. The measured data are represented later in this study.

According to the drop behavior, the mass transfer is described by two different particle models:

- Liquid oil drops are extracted as *shrinking particles* by convective mass transfer. The convection is dependent on the flow around a single particle. Thus, the flow dynamic in the spray cone is important. This flow is calculated by radial velocity profiles and the flow turbulence. Determination of the relative velocity between the spray particles and the fluid flow is possible with the momentum balance.
- In addition to the convective mass transfer there is a diffusive mass transfer inside of lecithin particles that form a solid shell around the unextracted core. Such particles are modeled with *a constant size and a shrinking unextracted core.* A porous structure of phospholipids in the shell is assumed for lecithin, while the shrinking core keeps the initial lecithin composition. The binary diffusion coefficient of oil in supercritical CO_2 can be calculated by the theory of the rough hard sphere, which is presented by Erkey et al. (1990).

For both particle models the driving force of the mass transfer is the concentration gradient between the phase boundary (surface of the liquid drop or of the shrinking unextracted core) and the bulk fluid. Saturation of the fluid according to the solubility measured by Friedrich (1984) and Quirin (1982) is assumed at the phase boundary, while the oil concentration in the fluid results from the coupled mass balance between the particles and the fluid phase.

Properties of the Model Substances

Surface tension in CO_2

Eggers and Wagner (1993) measured the decreasing effect of high pressure on the surface tension of lecithin in CO_2 at 348 K and pressures up to 27.5 MPa. The application of the pendant-drop method for these measurements, as described in detail by Eggers and Jaeger (1994), was carried out by photographing the drop in a high-pressure optical cell and evaluating the contour with a microscope. At present, measurements are extended to pressures up to 70 MPa at three temperatures between 353 K and 393 K. The object of these investigations is to characterize the behavior of surface tension at pressures around the known turning point (~ 35 MPa) in temperature dependency of solubility between oil and CO_2, as presented in Quirin (1982).

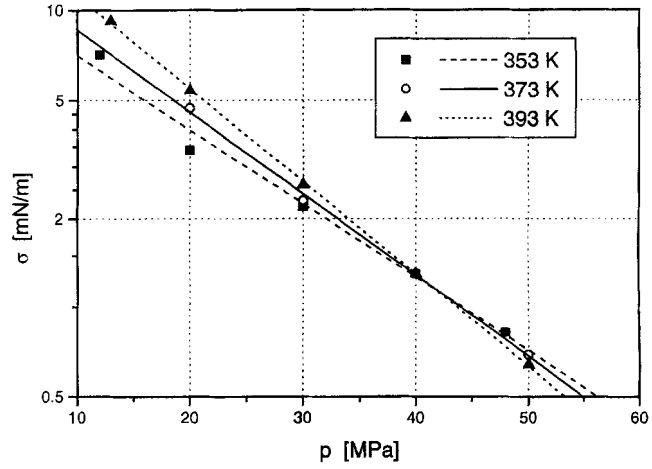

Figure 5. Surface tension of vegetable oils in supercritical CO_2.

The size of the pendant drop can be determined using a computerized image-analyzing system equipped with a video camera that generates high-resolution pictures with squared pixels. A frame grabber digitizes the pixel image synchronously, so that there are no distortions in the drop image.

Jaeger et al. (1995) report that systems of different vegetable oils show an equal surface tension in supercritical CO_2. These surface tensions are the same as the one measured for lecithin. Therefore the measurements in this study represent crude oil as well as lecithin.

Figure 5 shows the measured data up to 50 MPa in a logarithmic scale. The linear regressions represent an exponential decrease in surface tension. Different slopes of the straight lines result in an intersection between 35 and 45 MPa. The expected behavior of surface tension decrease with increasing solubility could be proved for pressures lower than 35 MPa. At pressures above 50 MPa, the error in the method prevents the measurement of a clear temperature dependency. At these pressures, a temperature-independent exponential function is used to correlate the surface tension in the temperature range 373 to 413 K:

$$\sigma\left[\frac{mN}{m}\right] = 0.27075 + 0.75016 \cdot \exp\left(-\frac{(p[\mathrm{MPa}] - 43.30457)}{10.45313}\right). \quad (1)$$

All the surface-tension data are valid for the saturation state. Lecithin cannot be measured in unsaturated CO_2 because it would form a solid structure instead of a pendant drop. But for oil in CO_2 the dynamic behavior of the pendant drop during the saturation process is given by Jaeger et al. (1995).

Viscosity of liquids mixed with CO_2

Some tests at temperatures of 333 K and 373 K could be carried out in a high-pressure rotational viscometer, which works the same as a Searle system. Temperatures above 373 K cause thermal damage to the lecithin during the sustained measurements. Only the short residence times and the oxy-

gen-free atmosphere in the extraction zone prevent such damage in the extraction process. Unfortunately, the viscosity of the oil is not enough to be measured in the rotational viscometer. According to published data on lecithin by Eggers and Wagner (1993) and on soy oil by Pryde (1980) and Swern (1979), the sharp decrease in viscosity at temperatures increase occurs at atmospheric pressure. Both dependencies can be correlated with the Vogel equation given by Reid et al. (1987):

$$\eta_0[\text{mPa}\cdot\text{s}] = k1\cdot\exp\left(\frac{k2}{k3+T}\right), \tag{2}$$

with

Parameter	Crude Oil	Lecithin
$k1$ [mPa·s]	0.06566	3.341
$k2$ [K]	1,010.65	648.66
$k3$ [K]	−143.62	−213.63

Current findings are focused on the influence of pressure and mixing with CO_2. Both dependencies could be measured for lecithin. The influence of pressure on the viscosity of lecithin without CO_2 can be described with the Bridgman correlation given by Reid et al. (1987) for liquid viscosities:

$$\eta_p = \eta_0\cdot\exp(k1\cdot p),$$

with

$$k1(333\text{ K}) = 0.0177\,\text{MPa}^{-1}$$
$$k1(373\text{ K}) = 0.0114\,\text{MPa}^{-1}. \tag{3}$$

The exponential increase in viscosity with an increase in pressure inhibits the break-up of drops, but a mixture of lecithin and CO_2 is formed inside the spraying device. A decrease in viscosity as the mixture ratio increases and the pressure influence on the viscosity of the mixture are shown in Figure 6. The curves start at the measured solubility point, which is in agreement with the solubilities of CO_2 in vegetable oils given by Klein (1988). As expected, the influence of the mixing ratio is much higher than the influence of the pressure.

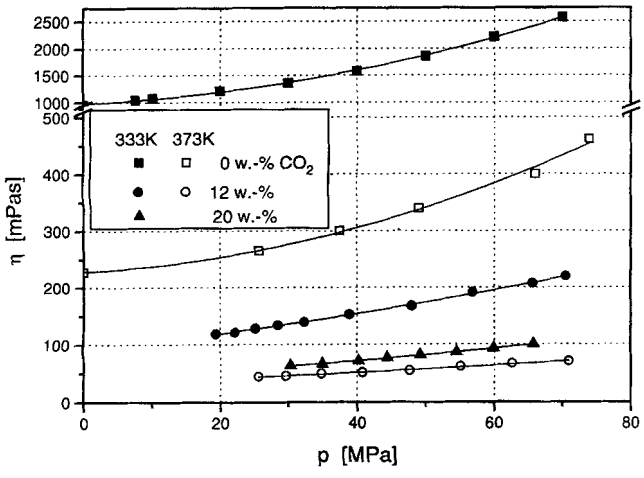

Figure 6. Viscosity behavior of lecithin mixed with CO_2.

Drop Formation in Fluid-Assist Spraying Devices

We used the measured and correlated liquid properties to determine the drop sizes generated in the spraying device. An overview of the atomization of liquids with air under atmospheric conditions is given by Lefebvre (1989). Drop-size distributions are characterized by the Sauter mean diameter. Correlations for the Sauter mean diameter are of the following form:

$$\frac{\bar{d}_S}{D_0} = k1\cdot\left(\frac{\sigma}{\rho_f\cdot v_{\text{rel}}^2\cdot D_0}\right)^{k2}\cdot\left(1+\frac{\dot{m}_l}{\dot{m}_f}\right)^{k3} + k4\cdot\left(\frac{\eta_l^2}{\sigma\cdot\rho_l\cdot D_0}\right)^{k5}\cdot\left(1+\frac{\dot{m}_l}{\dot{m}_f}\right)^{k6}. \tag{4}$$

Such correlations, with a summary of the influences caused by the atomizing fluid and by the liquid medium, have been found for the air-assist atomization under atmospheric conditions. Application of such correlations is not possible for atomization using supercritical fluids with a liquid-like density. The first addend describes the spraying force of the air. Because of the high fluid density, this leads to an improbably small diameter, from 2 to 25 μm. The influence of the liquid viscosity is determined by the second addend. For lecithin with an extremely high viscosity, this leads to a mean drop diameter that is in the range of several millimeters. Thus, the influence of the fluid momentum would be neglected by such an addition of the effects. Another disadvantage of this correlation is the use of mass flow rates, because they imply the velocity of gaseous air in the atomizer.

It is therefore necessary to find a correlation in which the influences of the fluid momentum and the liquid viscosity are accounted for by multiplication. Besides this, characteristic dimensionless numbers are useful when considering the flow dynamics inside of the atomizer.

To characterize the stability of liquid drops, the Weber number (We) is used as dimensionless number:

$$We = \frac{v^2\cdot\rho\cdot D}{\sigma} = \frac{\text{dynamic pressure by inertia}}{\text{internal pressure by surface tension}}. \tag{5}$$

According to Walzel (1990), a distinction must be made between the We number for the disintegration of a liquid filament in the nozzle and the gas-We-number (We_g) for the disintegration of drops in the gas stream. In the first case, the inertia of the liquid filament is expressed by its velocity and the liquid density, while for the gas-We-number it is expressed by the gas velocity and density of the gas stream.

The influence of the turbulence and the viscosity on the disintegration of a liquid filament can be described by the Ohnesorge number (Oh), which is defined as the quotient of the We and the Re numbers:

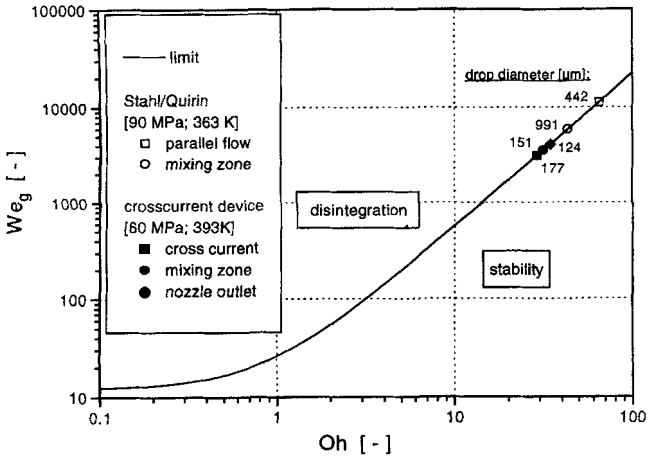

Figure 7. Drop disintegration limit according to Walzel (1990).

$$Oh = \frac{\sqrt{We}}{Re} = \frac{\eta_l}{\sqrt{\rho_l \cdot \sigma \cdot D}}. \quad (6)$$

Walzel (1990) gives a correlation that defines a drop-disintegration limit based on the limiting gas-*We*-number from the *Oh* number:

$$We_g = 12 + 14 \cdot Oh^{1.6}. \quad (7)$$

This disintegration limit is shown in Figure 7. The points on the graph represent the drop disintegration inside the mixing and extraction unit used by Stahl and Quirin (1985) on a laboratory scale compared to the conditions inside the crossflow spraying device on a semi-industrial scale used in this study. This comparison shows that drops with a diameter of 124 μm disintegrate when they leave the spraying device, while drops of nearly 1 mm are stable in the mixing device of Stahl and Quirin (1985). Thus, the definition of a drop-disintegration limit can only be used to estimate drop sizes.

To calculate the drop sizes formed in the spraying device used in this study, a correlation of Ingebo and Foster (1957) is used, wherein an *Re* number of the spraying process is defined:

$$Re_{SP} = \frac{v_f \cdot \rho_l \cdot D}{\eta_l} = \frac{\text{inertia of the fluid stream}}{\text{viscosity of the liquid}}. \quad (8)$$

The momentum exchange between the fluid flow and the liquid is determined by multiplying this *Re* number by the gas-*We*-number. The results of this multiplication are the same order of magnitude for spraying with dense CO_2 as for the system of kerosene and air, which was used to find the correlation. The Sauter mean diameter is given by the following expression:

$$\frac{\bar{d}_S}{D_0} = 3.9 \cdot (We \cdot Re_{SP})^{-0.25} \quad (9)$$

In addition to the correlation for the Sauter mean diameter, Ingebo and Foster (1957) modified a frequently used drop-size distribution by Nukiyama and Tanasawa (1939). The modified distribution function is given in differential form:

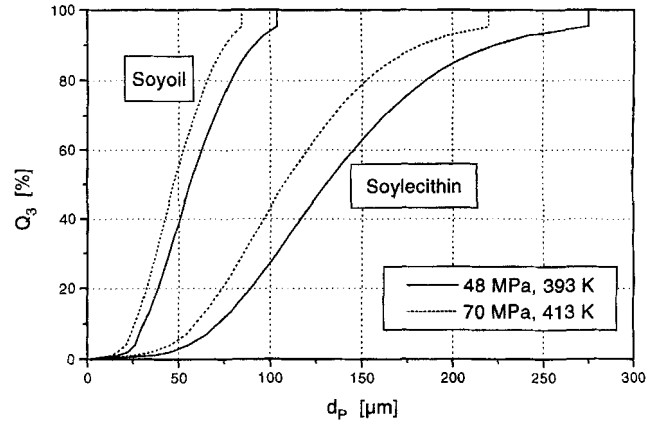

Figure 8. Drop-size distribution for spraying of liquids with supercritical CO_2.

$$\frac{dQ_3}{dd_P} = 10^6 \cdot (We \cdot Re_{SP})^{-0.24} \cdot \frac{d_P^5}{d_{P,\max}^6} \cdot \exp\left(-22.3 \cdot (We \cdot Re_{SP})^{-0.04} \cdot \frac{d_P}{d_{P,\max}}\right), \quad (10)$$

with

$$d_{P,\max} = 22.3 \cdot D_0 \cdot (We \cdot Re_{SP})^{-0.29}.$$

In the model this differential drop distribution is integrated and allowed for by discretization of the distribution curve, which is shown in Figure 8 for spraying lecithin and crude oil. The two graphs for each medium represent the bounds of drop sizes in the range of extraction conditions used. A maximum drop diameter in the distribution is considered. Such a maximum drop size is also given by Mugele and Evans (1951) as being characteristic for atomization processes.

For the atomization of lecithin the diameter of the drop distribution is in the range of 50 μm to 250 μm. The use of a high-pressure optical cell, as well as determining the raffinate by sedimentation velocity in supercritical CO_2 and by Ergun-analysis of air flow through fixed beds, shows particle sizes in this range. This proves that the correlation is applicable to atomization processes with dense gases.

Mass Balance

Single particle

The mass balance at a single particle depends on an extraction rate (Θ), which comes from the mass transfer and is related to the outside particle surface. When crude oil is extracted, the mass of an oil drop is consistent with the unextracted amount of oil. In contrast, the deoiling of solid lecithin particles can be described by use of the particle loading:

$$m_{s,P} \cdot X_P = m_{s,P} \cdot (X_P + dX_P) + \Theta \cdot A_P \cdot dt. \quad (11)$$

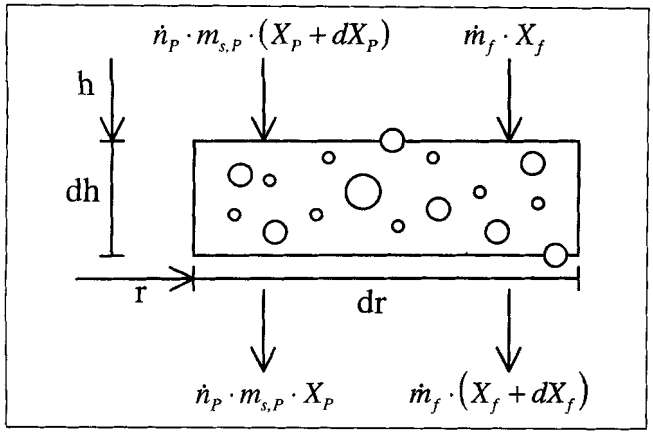

Figure 9. Mass balance in a differential volume.

Particle velocity can be used to determine the change in the oil loading of a particle over a differential height.

$$dX_P = -\Theta \cdot \frac{A_P}{m_{s,P}} \cdot \frac{dh}{v_P}. \tag{12}$$

The extraction rate of a shrinking drop can be determined by convective mass transfer (β) alone, but for solid particles with a shrinking unextracted core the diffusion inside the particle structure (D_{eff}) must be considered.

Differential fluid volume

A differential volume can be defined by differentiation in axial and radial directions. According to Figure 9, the particle and fluid loading of oil are connected, so that the change in particle loading causes a change in the fluid loading:

$$dX_f = \frac{\dot{n}_P \cdot m_{s,P}}{\dot{m}_{s,P}} \cdot dX_P. \tag{13}$$

For mathematical evaluations in the free jet and in the tube flow, a one-dimensional determination in axial direction is used. Because of inertia and the large velocity in axial direction, the particles are assumed to stay in fixed annular differential volumes. In the fluid phase radial, but not axial, mixing is assumed. This is consistent with the radial velocity profile of fully developed turbulent flow. Therefore, the oil concentration gradient necessary for the mass transfer between particle and fluid depends on the particle size and the radial position.

Mass Transfer from the Particle to the Fluid

Different mass transfer models must be used for liquid drops and solid particles. The convective mass transfer for liquid drops can be described by a transfer coefficient, which is calculated with a Sherwood function formulated by Ranz and Marshall (1952) for spherical particles in gas and liquid flows:

$$Sh = 2 + 0.6 \cdot Sc^{1/3} \cdot Re_P^{1/2}. \tag{14}$$

In this function the particle *Re* number depends on the relative velocity between particles and fluid flow in the extraction zone. This can be calculated by the fluid dynamics and the momentum balance.

The extraction of oil from solid particles is described by a shrinking particle model by convective mass transfer and diffusion in the particle structure. An overall mass-transfer coefficient is considered for the extraction rate:

$$k_{mt} = \frac{1}{\frac{1}{\beta} + \frac{d_P}{2 \cdot D_{\text{eff}}} \cdot \left(\frac{d_P}{d_i} - 1 \right)}. \tag{15}$$

Observations with a high-pressure optical cell show that lecithin drops from hard-shelled particles after leaving the spraying device. While drops become hard-shelled particles, pure convective mass transfer is presumed. But because the deoiled parts of the particle show a flocculent structure, the outside flow is assumed to even reach into the hollow spaces of the outer layers and cause an extension of the convective mass-transfer regime. When the particle's extraction front is at a depth the convective flow cannot reach, diffusion begins in the overall mass transfer resistance. The penetration depth of the outside fluid flow corresponds to the change from convective to overall mass transfer; it is therefore used as one adaption parameter in the model.

The binary diffusion coefficient of oil in supercritical CO_2 is calculated by correlations based on the rough-hard-sphere-theory by Erkey et al. (1990). Two effects hinder diffusion inside the particle structure. First, diffusion can occur only in the void part of the particle, and second, the diffusion path is extended by the irregularity of the pores. Both effects are considered in a correlation, described by Keil (1993), that Wheeler used to find the coefficient for the effective diffusion:

$$D_{\text{eff}} = \frac{\epsilon}{\tau^2} \cdot D_{12}. \tag{16}$$

The void part inside the extracted particle is calculated by the fraction of oil and phospholipids in the lecithin, while the irregularity is used as a second adaption parameter to describe the particle structure.

Fluid Dynamics

The relative velocity between the two phases in the spray cone and in the tube are especially interesting to the convective mass transfer. The liquid drops or solid particles are accelerated in the fluid flow. First, a model for the radial velocity profiles is necessary. Once the fluid velocity is known, the acceleration of particles can be determined by the momentum balance between the two phases, so that the difference between the two velocities can be calculated from the distance to the spraying device. The relative velocity between fluid and particles decreases with the flow condition of the two-phase flow. Thus the influence of the turbulent fluctuation on the fluid flow increases and must be considered for the convective mass transfer. The view is restricted to one dimension, namely to the axial component of these velocities.

Radial velocity profiles

The fluid flow in the extraction zone has three different regions in the axial direction. First a *spray cone* with a continuous diameter expansion is formed at the orifice edge of the spraying device. Therefore the radial velocity profile changes in relation to the distance to the spraying device. Where the spray cone reaches the tube wall, the radial velocity profile shows a transition into the turbulent tube flow. The second region is called *flow transition*, and the third is a *turbulent tube flow*, which occurs in the remaining tube length. The extraction of liquid drops should occur in an extraction region in which only a spray cone is formed. Contrarily, solid particles can run through all three regions.

The spray cone is seen as a free jet, except that here no additional amount is carried out of the ambient gas. Thus, the free jet velocity profile, which is known from fundamental fluid dynamics, must be adjusted in regard to the constant volume flow. In addition to this adjustment, a certain amount of the free jet profile is outside the tube wall. The portion of the free jet that is outside the tube needs to be added to the inside velocity profile to keep the volume flow constant. A velocity profile like the following results:

$$v(x,r) = 31.105 \cdot v_0 \cdot \frac{D_0^2}{x^2} \cdot \left(1 + 124.42 \cdot \frac{r^2}{x^2}\right)^{-2} + \frac{v_0 \cdot D_0}{D^2 \cdot \left(1 + 31.105 \cdot \frac{D^2}{x^2}\right)}. \quad (17)$$

With increasing distance, this free jet velocity profile is more like the profile of a fully developed turbulent flow. Turbulent velocity profiles in a tubular flow are also known from fundamental fluid dynamics. According to Nikuradse (1932), the following expression can approximate it by *Re* numbers lower than 10^5:

$$v_{\text{turb}}(r) = v_{\text{turb,max}} \cdot \left(\frac{R - r}{R}\right)^{1/7}$$

with

$$v_{\text{turb,max}} = 1.224 \cdot \bar{v}_{\text{turb}} = 1.224 \cdot \frac{\dot{V}}{\pi \cdot R^2}. \quad (18)$$

The pipe flow profile is assumed from the point of minimal deviation between the free jet and the turbulent pipe flow. The development of the radial velocity profile is shown in Figure 10 for the extraction tube with a diameter of 14.3 mm at distances from the spraying device of 50 mm to the point of minimal deviation between the velocity profiles. The velocity is given relative to the outlet velocity of the spraying device.

Momentum balance in the two-phase flow

To determine the relative axial velocity between the particles and the fluid flow, the momentum balance is solved for the axial direction by considering the following forces:

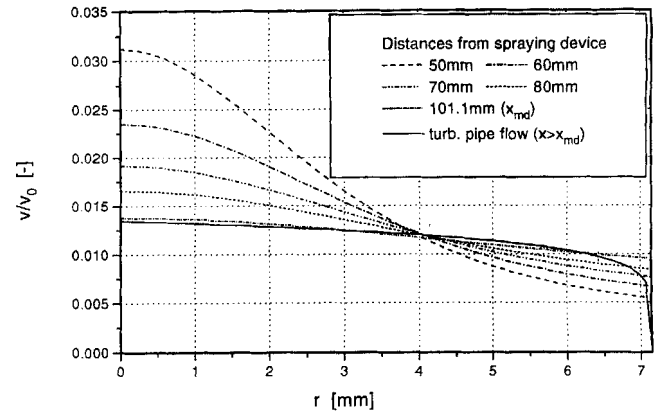

Figure 10. Radial velocity profile at different distances to the spraying device.

Gravity: $F_G = \rho_P \cdot V_P \cdot g$

Buoyancy: $F_B = -\rho_F \cdot V_P \cdot g$

Inertia: $F_I = -\rho_P \cdot V_P \cdot a$

Drag: $F_R = -\rho_F \cdot |v_{\text{rel}}| \cdot v_{\text{rel}} \cdot A \cdot c_W$.

The equilibrium of forces ($\Sigma F_j = 0$) give the differential change of particle velocity:

$$\frac{dv_P}{dh} = g \cdot \frac{\rho_P - \rho_F}{\rho_P \cdot v_P} \pm \frac{3}{4} \cdot \frac{\rho_F \cdot c_w}{\rho_P \cdot d_P} \cdot \frac{(v_F - v_P)^2}{v_P}. \quad (19)$$

Inside the spraying device, the flow generates and accelerates (summation) drops. In the spray cone the fluid velocity decreases, so there is a moderating (subtraction) effect on the particle velocity. Inside the tubular extraction zone, the particles are assumed to stay in differential annular segments.

Turbulent fluctuation of the fluid flow

The turbulent fluctuation in the fluid flow around a particle increases the relative velocity between the particle and the fluid. When the two velocities are equalized, this is the only effect that causes a convective mass transfer.

A way of determining the axial fluctuation comes from Prandtl's theory of eddy mixing length, which is described by Davies (1972). Therefore the fluctuation is found by multiplying the eddy mixing length by the derivation of the velocity profile:

$$v_x'(r) = l_{Pr} \cdot \frac{1}{7} \cdot \left(\frac{R - r}{R}\right)^{-6/7} \cdot v_{\text{turb,max}}. \quad (20)$$

The eddy mixing length can be approximated from measurements by Nikuradse (1932). In relation to the maximum velocity, the axial fluctuation is between 2% on the tube axis and 6% near the tube wall, as shown in Figure 11.

The sum of this axial fluctuation and the relative axial velocity from the momentum balance is used to describe the flow around a particle in the Sherwood correlation (*Sh*) for the convective mass transfer.

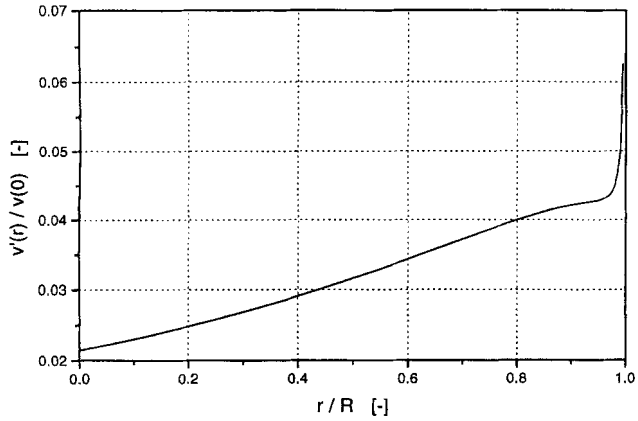

Figure 11. Axial fluctuation in a turbulent tube flow.

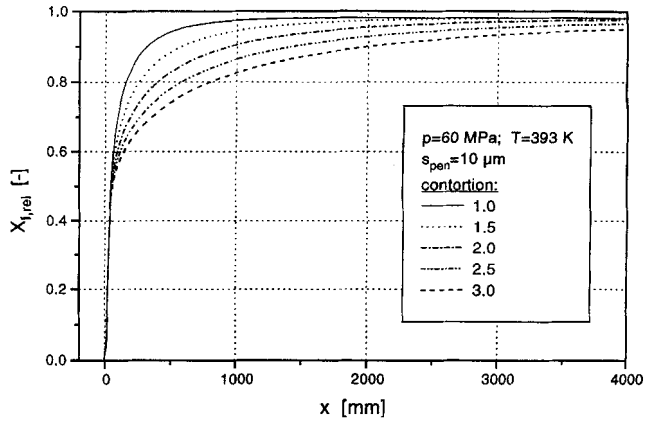

Figure 13. Influence of the distortion on the extraction-rate profile.

Calculation of Concentration Profiles

After using the model described in the preceding sections in a differential calculation on a workstation (HP-Apollo, Series 700) over the three different flow regions in the extraction zone, an axial extraction rate profile was determined. For the case of the deoiling of lecithin, this profile could be adapted to oil concentrations in the fluid phase measured in the extraction zone by sampling at distances of 0.3 and 1 m from the spraying device. These concentrations depend on the following parameters: pressure, temperature, fluid mass flow, and mass flow ratio (liquid/fluid). The depth of penetration in the outside fluid flow and the distortion inside the particle are used as adaption parameters for the model. Both parameters describe structural phenomena of the particles. Figure 12 shows that a variation in the penetration depth varies the degree of extraction, which is reached before diffusion begins having a significant effect on the mass transfer. In comparison, according to Figure 13, the distortion varies the diffusional influence on the overall mass transfer.

If the concentration in the fluid is related to the concentration for complete deoiling, the mass flow ratio has nearly no influence on the concentration profile. Thus it is possible to adapt the profile to the average relative concentration of several measurements at different mass flow ratios. Such adaptions are shown in Figure 14 for two model extraction conditions. Every point represents approximately 10 measurements. Altogether, concentration profiles at pressures of 48, 60, and 70 MPa, and at temperatures of 373, 393, and 413 K, have been used for model adaptions.

For all these conditions it is possible to adapt the concentration profiles with constant adaption parameters. So, as expected, the structural parameters of the particle are independent of the extraction condition. Obviously, the model is suitable for describing the drop formation and the mass transfer in two-phase flows with supercritical fluids.

By way of comparison, calculated concentration profiles are given for the extraction of oil drops at matching conditions. These show that, in spite of the better mass transfer, the drops cannot be extracted in a tube with a diameter of only 14.3 mm. In such a tube the spray cone hits the wall after 45 mm, but a complete drop extraction is not reached until 100 to 140 mm. Corresponding to this calculation, successful deslimming of crude oil could be carried out in the extraction zone with the wider diameter of 50 mm and a spray cone length of about 200 mm.

Conclusion

The idea of decreasing the mass-transfer resistance in liquid phases by an extreme reduction of the diffusion paths,

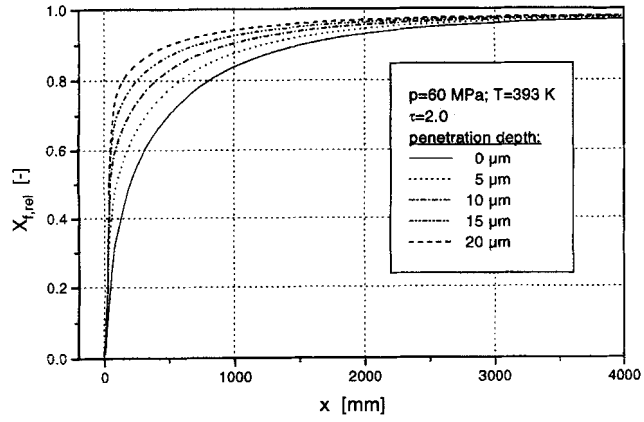

Figure 12. Influence of the penetration depth on the extraction-rate profile.

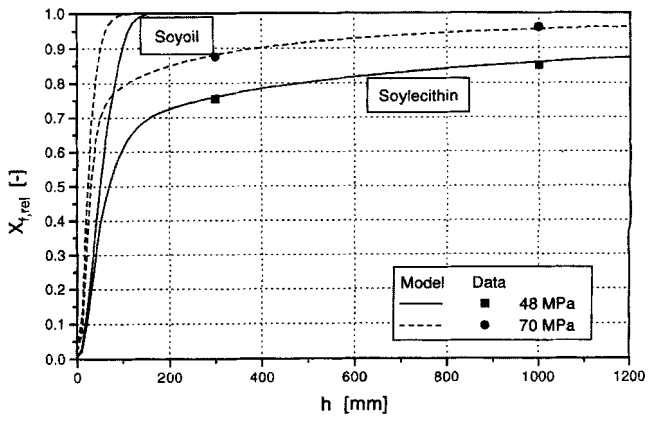

Figure 14. Adaption of the concentration profile to the measurements.

with a simultaneous increase in mass transfer surface, was realized in supercritical systems by spraying a liquid along with the dense fluid and extracting the spray particles in the resulting two-phase flow. In this work, the spraying and extraction of liquid materials with supercritical CO_2 was described by a mathematical model. Fundamental formulations for the particle formation in atomizers, the fluid dynamics, and the mass transfer in turbulent two-phase flows were successfully modified to match the problem of supercritical fluid extraction. So, the model requires only the properties of the process media and, if solids are formed during the extraction, two independent parameters describing their material structure.

The drop-size distribution for the spraying device and the concentration profile in a given extraction zone were determined. These results can be used to optimize the apparatus used in the two process steps, "mixing" (spraying) and "loading" (extraction).

Notation

a = acceleration
A = area
c_w = resistance factor
d = particle diameter
D = apparatus diameter
D_{12} = diffusion coefficient
h = height
k_{ml} = overall mass-transfer coefficient
l_{Pr} = eddy mixing length (Prandtl's theory)
m = mass
n = number
p = pressure
Q_3 = volume fraction in drop-size distribution
r = radius
R = radius of the extraction zone
t = time
T = temperature
v = velocity
$\dot{V}$ = volume flow
x = distance
X = loading

Greek letters

β = mass-transfer coefficient
ϵ = void fraction
η = dynamic viscosity
ρ = density
σ = surface tension
τ = contorsion
θ = extraction rate

Subscripts

0 = at the outlet of the spraying device or at normal conditions
f = fluid phase
i = inside
l = liquid phase
md = minimal deviation
p = under pressure
P = particle
s = solid

Literature Cited

Chung, T.-H., M. Ajlan, L. L. Lee, and K. E. Starling, "Generalized Multiparameter Correlation for Nonpolar and Polar Fluid Transport Properties," *Ind. Eng. Chem. Res.*, **27**, 671 (1988).

Davies, J. T., *Turbulence Phenomena*, Academic Press, New York (1972).

Eggers, R., and H. Wagner, "Extraction Device for High Viscous Media in a High Turbulent Two-Phase Flow with Supercritical CO_2," *J. Supercrit. Fluids*, **6**, 31 (1993).

Eggers, R., and Ph. T. Jaeger, "Der Einfluß von Grenzflächenerscheinungen auf den Stoffübergang und die Prozeßführung in Gegenstromkolonnen mit überkritischem CO_2," *Wärme Stoffübertrag.*, **29**, 373 (1994).

Erkey, C., H. Gadalla, and A. Akgerman, "Application of Rough Hard Sphere Theory to Diffusion in Supercritical Fluids," *J. Supercrit. Fluids*, **3**, 180 (1990).

Friedrich, J. P., "Supercritical CO_2 Extraction of Lipids from Lipid-Containing Materials," U.S. Patent 4,466,923 (Aug. 21, 1984).

Ingebo, R. D., and H. H. Foster, "Drop-Size Distribution for Cross-current Breakup of Liquid Jets in Airstreams," NACA Tech. Note 4087 (Oct. 1957).

Jaeger, Ph. T., J. von Schnitzler, and R. Eggers, "Interfacial Tension of Fluid Systems Considering the Nonstationary Case with Respect to Mass Transfer," *Chem. Eng. Technol.*, **18** (1996).

Keil, F., "Diffusion und chemische Reaktion in der Gas/Feststoff-Katalyse," *Chem. Tech.*, **45**, 437 (1993).

Klein, T., "Phasengleichgewichte in Gemischen aus pflanzlichen Ölen und Kohlendioxid," *Fortschr. Ber. VDI*, **3**(159), VID-Verlag, Düsseldorf (1988).

Lefebvre, A. H., *Atomization and Sprays*, Hemisphere, New York (1989).

Mugele, R. A., and H. D. Evans, "Droplet Size Distribution in Sprays," *Ind. Eng. Chem.*, **43**, 1317 (1951).

Nikuradse, J., "Gesetzmäßigkeiten der turbulenten Strömung in glatten Rohren," *VDI-Forschungsheft*, No. 356 (1932).

Nukiyama, S., and Y. Tanasawa, "An Experiment on the Atomization of Liquid," *Trans. Soc. Mech. Eng. (J.)*, **5**, 68 (1939).

Pryde, E. H., "Physical Properties of Soybean Oil," *Handbook of Soy Oil Processing and Utilization*, American Soybean Association and American Oil Chemists' Society (1980).

Quirin, K.-W., "Löslichkeitsverhalten von fetten Ölen in komprimiertem Kohlendioxid im Druckbereich bis 2600 bar," *Fette, Seifen, Anstrichmm.*, **84**, 460 (1982).

Ranz, W. E., and W. R. Marshall, "Evaporation from Drops," *Chem. Eng. Prog.*, **48**, 141 (1952).

Reid, R. C., J. M. Prausnitz, and B. E. Poling, *The Properties of Gases and Liquids*, McGraw-Hill, New York (1987).

Sievers, U., "Die thermodynamischen Eigenschaften von Kohlendioxid," *Fortschr. Ber. VDI-Z.*, **6**(155), VDI-Verlag, Düsseldorf (1984).

Stahl, E., and K.-W. Quirin, "Entölung von Rohlecithin durch Hochdruck Düsenextraktion mit Kohlendioxid," *Fette, Seifen, Anstrichmm.*, **87**, 219 (1985).

Swern, D., ed., *Bailey's Industrial Oil and Fat Products*, Wiley, New York, Chap. 3, p. 177 (1979).

Walzel, P., "Zerstäuben von Flüssigkeiten," *Chem. Ing. Tech.*, **62**, 983 (1990).

Manuscript received July 19, 1995, and revision received Oct. 30, 1995.